Supplementary Information

All-site alloyed perovskite for efficient and bright blue light-emitting diodes

Yu Chen[1], Ruishan Wang[1], Gunnar Kusch[2], Bo Xu[1], Chenjie Hao[1], Chen Xue[1], Lu Cheng[3], Lin Zhu[1], Jingmin Wang[1], Hai Li[1], Rachel A. Oliver[2], Nana Wang[1]*, Wei Huang[1,4,5]*, Jianpu Wang[1,6]*

[1]State Key Laboratory of Flexible Electronics (LoFE) & Institute of Advanced Materials (IAM), School of Flexible Electronics (Future Technologies), Nanjing Tech University (NanjingTech), Nanjing 211816, China.

[2]Department of Materials Science and Metallurgy, University of Cambridge, 27 Charles Babbage Road, Cambridge CB3 0FS, UK.

[3]School of Microelectronics & Data Science, Anhui University of Technology, Ma'anshan 243002, China.

[4]Shaanxi Institute of Flexible Electronics (SIFE), Xi'an Institute of Biomedical Materials & Engineering (IBME), Northwestern Polytechnical University (NPU), 127 West Youyi Road, Xi'an 710072, China.

[5]Strait Laboratory of Flexible Electronics (SLoFE), Fujian Normal University, Fuzhou 350117, China.

[6]The Materials and Electronics Research Center (MERC), School of Materials Science and Engineering and School of Microelectronics and Control Engineering, Changzhou University, Changzhou 213164, China.

Corresponding authors: iamjpwang@njtech.edu.cn, vc@nwpu.edu.cn, iamnnwang@njtech.edu.cn.

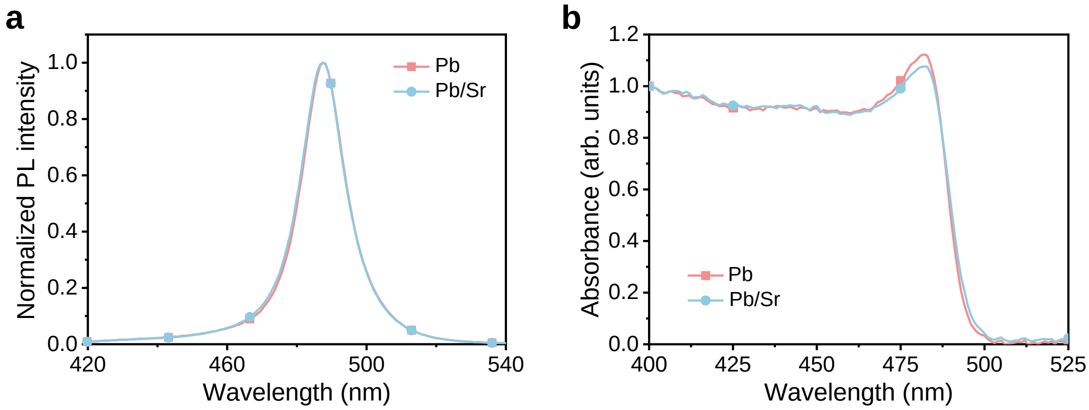

Supplementary Fig. 1 Characterizations of Pb and Pb/Sr blue perovskite films. a, PL spectra of blue perovskite films. **b**, Absorption spectra of blue perovskite films.

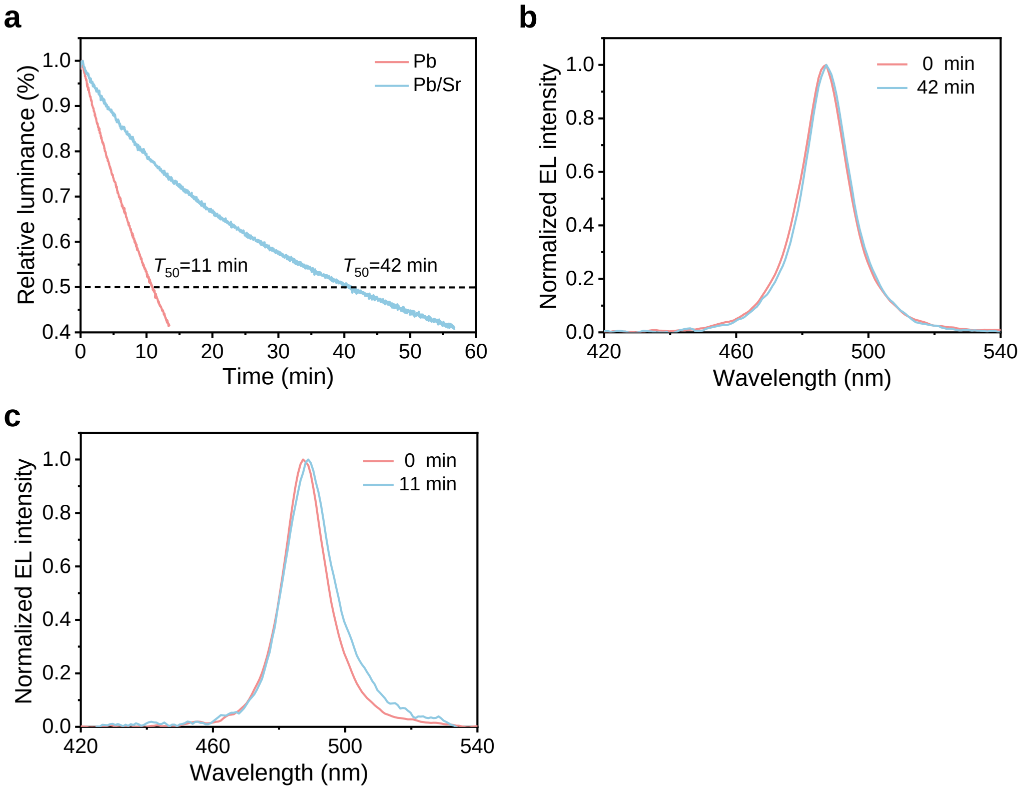

Supplementary Fig. 2 Stability characterization of blue perovskite LEDs. a, Stability data of devices measured at an initial luminance of 50 cd m^{-2} (near the peak EQE position). **b,c**, EL spectra of Pb/Sr device (**b**) and Pb device (**c**) during stability measurement. The EL spectra of the Pb/Sr perovskite LED show minimal change after aging for 42 min, while the Pb perovskite LED exhibits a significant red-shifted and broadening spectrum after aging for 11 min.

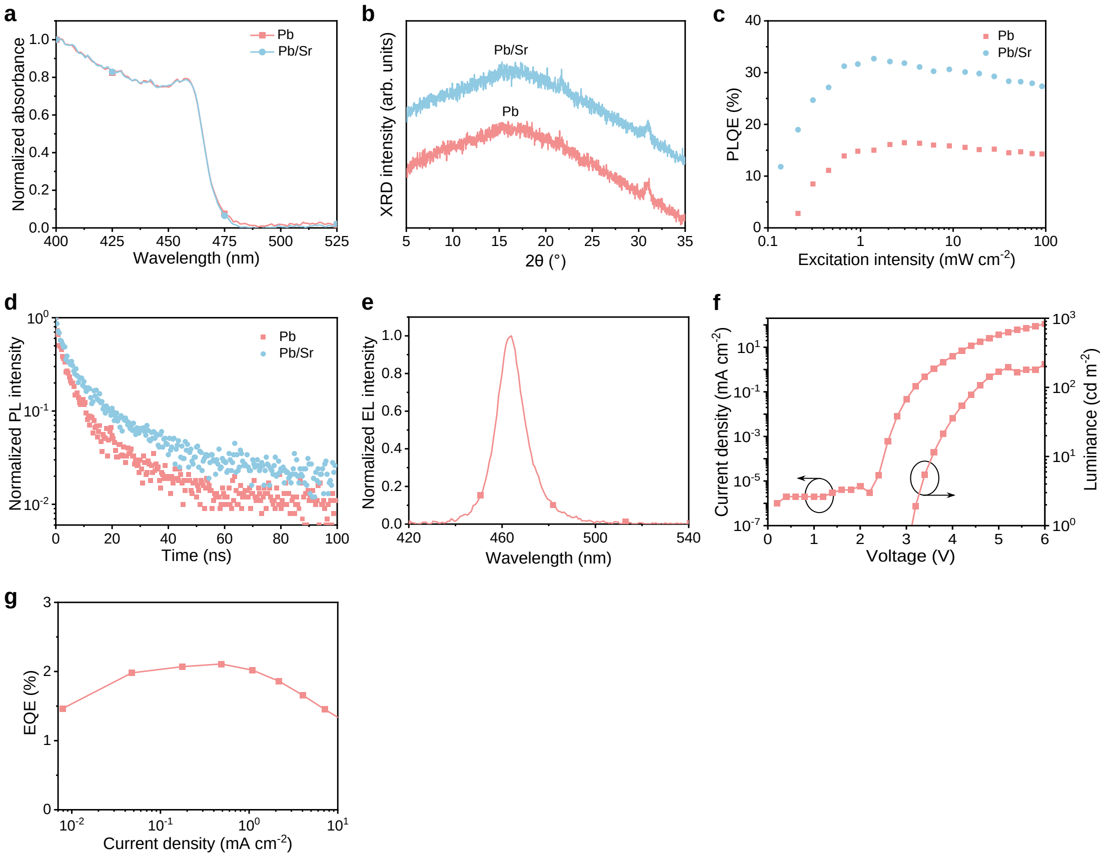

Supplementary Fig. 3 Characteristics of deep-blue (464 nm) perovskite films and LEDs. a, Absorption spectra of the deep-blue perovskite films, showing no absorption peaks from low-dimensional perovskites. **b**, XRD patterns of the deep-blue perovskite film. There are no diffraction peaks from low-dimensional perovskites, suggesting that the deep-blue perovskites are 3D crystals. **c**, Excitation-intensity-dependent PLQEs. **d**, Transient PL decays of Pb or Pb/Sr perovskites at a carrier density of 1.7×10^{15} cm^{-3}. **e**, EL spectrum of the device without $SrBr_2$. **f**, Current density and luminance versus voltage of the device without $SrBr_2$. **g**, Dependence of the EQE on the current density of the device without $SrBr_2$.

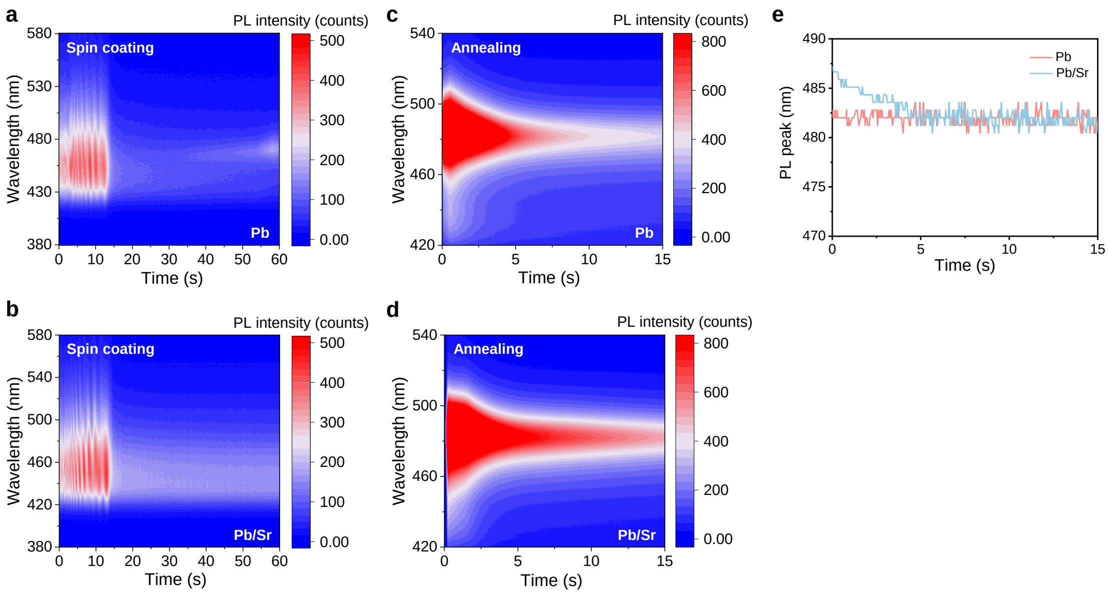

Supplementary Fig. 4 In situ PL measurements of perovskites during the growth process. a,b, Contour plot of PL spectra of Pb (**a**) and Pb/Sr (**b**) perovskites during the spin-coating process. **c,d**, Contour plot of PL spectra of Pb (**c**) and Pb/Sr (**d**) perovskites during the initial 15 s annealing process. The reduction of PL intensity is due to thermal quenching, while the Pb/Sr perovskite can maintain higher PL intensity. **e**, PL peak position extracted from in situ PL measurements of perovskites during the initial 15 s annealing process.

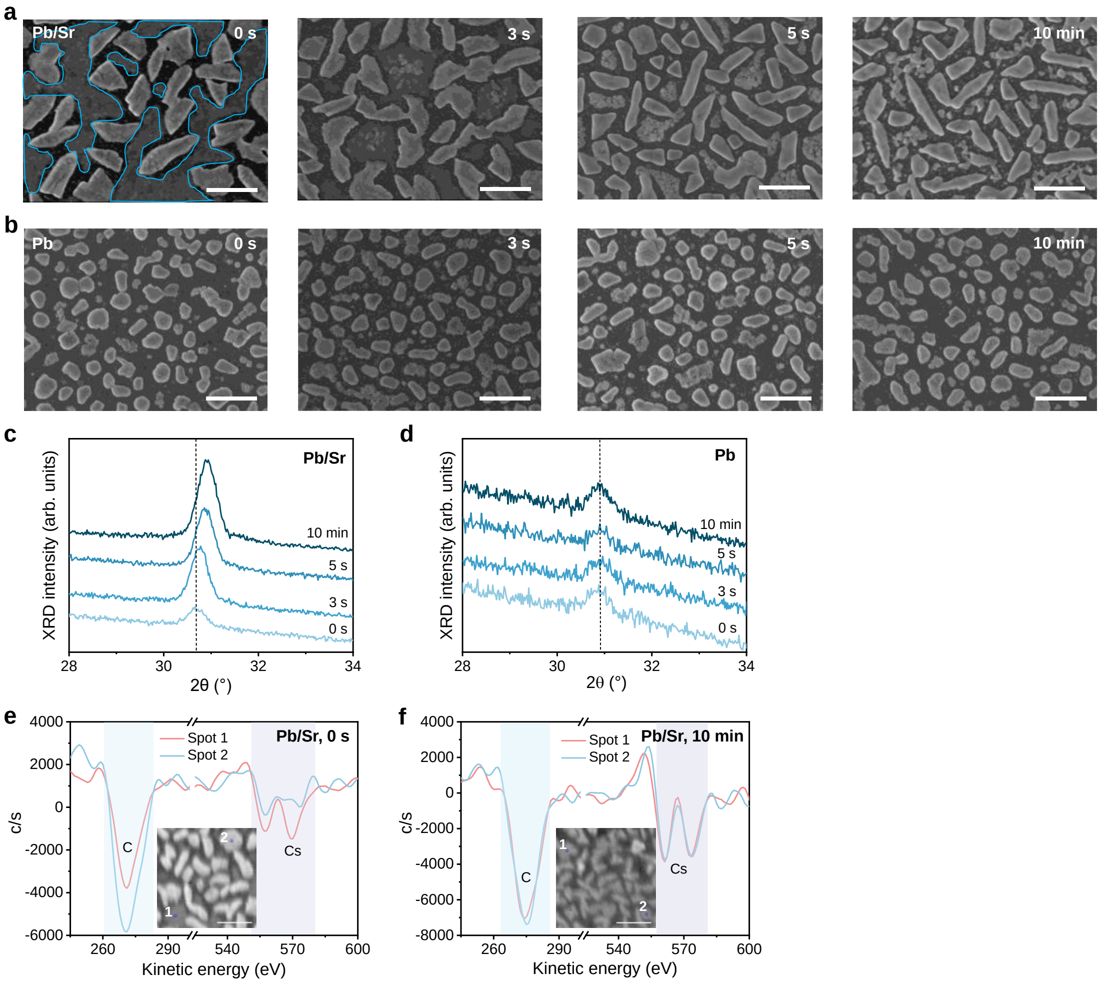

Supplementary Fig. 5 Characterization of perovskite films with different annealing times. a,b, SEM images of Pb/Sr (**a**) and Pb (**b**) perovskites. The 'mud bank-like' areas in the 0 s Pb/Sr perovskite film are circled by blue lines. The Pb perovskite films maintain similar morphology during the annealing process. Scale bar, 500 nm. **c,d**, XRD patterns of Pb/Sr (**c**) and Pb (**d**) perovskites. All Pb perovskites exhibit a diffraction peak at 30.9°. **e,f**, Analysis of C and Cs elements for AES measurements of Pb/Sr perovskites annealed for 0 s (**e**) and 10 min (**f**). It shows that the large grain in the as prepared perovskite is FA-rich phase, and the 'mud bank-like' part is Cs-rich phase. After being annealed for 10 min, the perovskite grains exhibit similar C and Cs signals, suggesting a uniform distribution of perovskites. Scale bar, 1 μm.

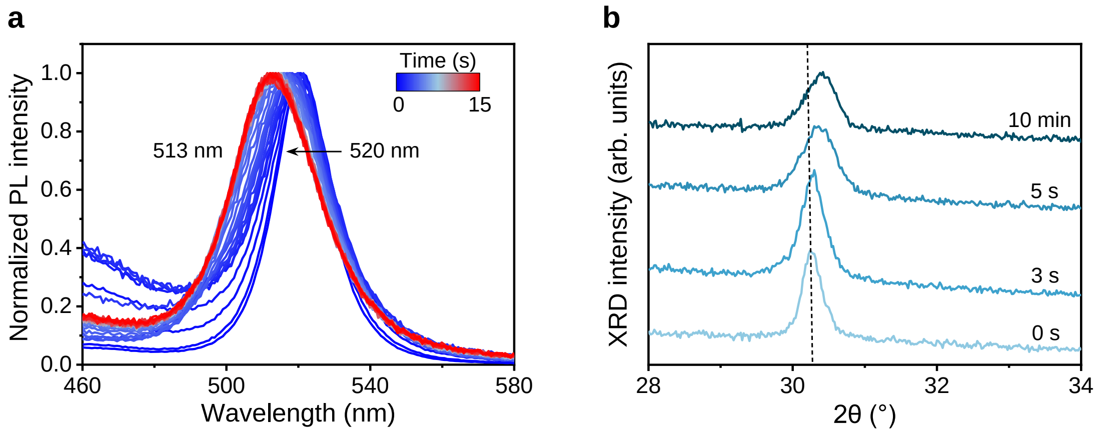

Supplementary Fig. 6 Characterization of (FA/Cs/Rb)(Pb/Sr)Br_3 perovskite film with different annealing times. a, Normalized PL spectra. The perovskite shows a blue-shifted PL peak with increasing annealing time. **b**, XRD patterns. As the annealing time increases, the XRD peak at 30.3° gradually shifts to a larger diffraction angle at 30.4°.

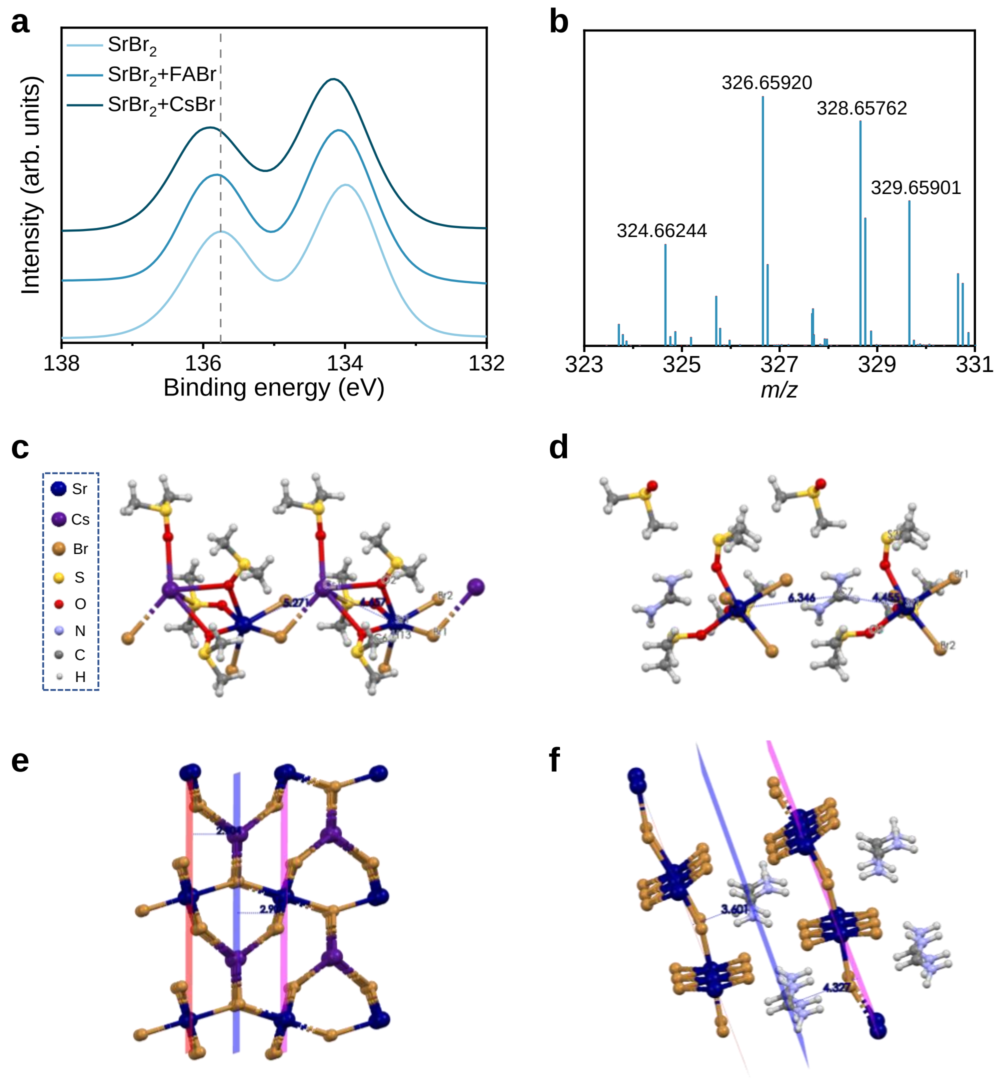

Supplementary Fig. 7 Understanding the interaction between CsBr and $SrBr_2$. a, XPS spectra. Upon addition of FABr or CsBr to $SrBr_2$, the Sr 3*d* peaks exhibit a shift to higher binding energy by 0.1 eV and 0.2 eV, respectively. **b**, ESI-TOF-MS spectrum of $SrBr_2$ solution in DMSO. The $SrBr_2$ solution shows typical $[SrBr_3]^-$ peaks. **c,d**, Schematic illustration of interactions between Sr^{2+}-based anions and Cs^+ (**c**) or FA^+ (**d**) cations in the solvent environment with $[SrBr_3]^-$. **e,f**, Schematic illustration of interactions between Sr^{2+}-based anions and Cs^+ (**e**) or FA^+ (**f**) cations in the solid-state structures.

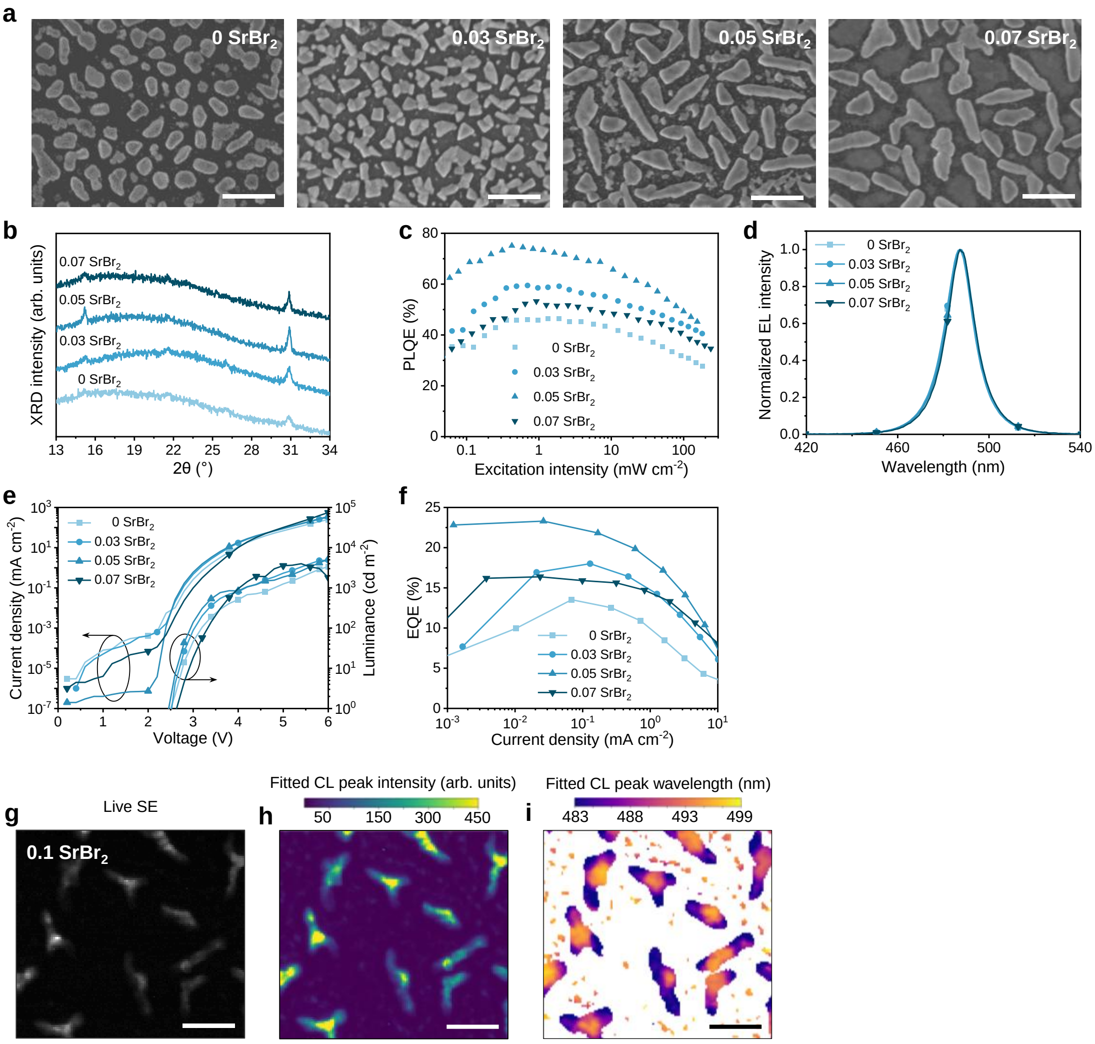

Supplementary Fig. 8 Characterization of perovskite films and LEDs prepared with various $SrBr_2$ amounts. a, SEM images. Scale bar, 500 nm. **b**, XRD patterns. **c**, Excitation-intensity-dependent PLQEs. **d**, EL spectra. **e**, Dependence of the current density and luminance on the driving voltage. **f**, EQE versus current density. **g-i**, Cathodoluminescence characterizations of perovskite film with a 0.1 ratio of $SrBr_2$. Scale bar, 700 nm. SEM image (**g**), corresponding CL peak intensity (**h**), and CL peak wavelength map (**i**).

Supplementary Table 1 Comparison of our devices with other high-performance blue perovskite LEDs with PL peak below 490 nm.

Perovskite	EL peak (nm)	CIE	EQE (%)	L_{max} (cd m^{-2})	Luminous efficacy (lm W^{-1})	Reference
3D perovskite	487	(0.070, 0.246)	23.3	5,700	33.4	Our work
3D perovskite	487	(0.096, 0.119)	13.6	18,748	–	[1]
3D perovskite	482	(0.09, 0.17)	19.28	1,457	–	[2]
3D perovskite	468	(0.126, 0.061)	11.9	668	7.33	Our work
3D perovskite	464	(0.132, 0.046)	7.5	317	3.87	Our work
3D perovskite	463	(0.136, 0.046)	4.1	150	–	[3]
Quasi-2D perovskite	488	(0.084, 0.283)	14.2	4,700	17	[4]
Quasi-2D perovskite	488	(0.074, 0.277)	21.6	10,030	–	[5]
Quasi-2D perovskite	488	(0.085, 0.230)	23.6	~1,000[a)]	–	[6]
Quasi-2D perovskite	483	(0.090, 0.180)	21.4	1,981	–	[7]
Quasi-2D perovskite	478	(0.106, 0.134)	21.9	640	–	[8]
Quasi-2D perovskite	469	(0.13, 0.06)	10.4	2,428	–	[9]
Quasi-2D perovskite	459	(0.136, 0.051)	15.36	~120[a)]	–	[10]
Perovskite NCs	480	(0.085, 0.205)	26.4	1,601	–	[11]
Perovskite NCs	478	(0.11, 0.13)	17.9	2,910	–	[12]
Perovskite NCs	465	(0.127, 0.069)	16.7	430	–	[11]
Perovskite NCs	460	(0.138, 0.045)	12	255	–	[11]

[a)]This data was estimated from the figures in the reference.

Supplementary References:

1. Xiong, W. *et al.* Efficient and bright blue perovskite LEDs enabled by a carbazole-phosphonic acid interface. *ACS Energy Lett.* **8**, 2897–2903 (2023).
2. Liu, A. *et al.* Optimizing perovskite surfaces to enhance post-treatment for efficient blue mixed-halide perovskite light-emitting diodes. *Adv. Mater.* (2024) doi: 10.1002/adma.202414788.
3. Jia, Y. *et al.* Unveiling the complex evolution in mixed Br–Cl perovskite precursors for high-efficiency deep-blue light-emitting diodes. *Small Struct.* **4**, 2200393 (2023).
4. Wang, Z. *et al.* Defect passivation efficacy of 2D perovskite interlayer for perovskite sky-blue emission toward high device efficiency. *Adv. Funct. Mater.* **34**, 2310389 (2024).
5. Jiang, M., Zhang, X. & Wang, F. Efficient perovskite nanograin light-emitting diodes in green-to-blue gamut with co-additive engineering. *Adv. Mater.* **36**, 2400565 (2024).
6. Zhang, K. *et al.* Nondestructive halide exchange via S_N2-like mechanism for efficient blue perovskite light-emitting diodes. *Nat. Commun.* **15**, 10621 (2024).
7. Yuan, S. *et al.* Efficient blue electroluminescence from reduced-dimensional perovskites. *Nat. Photonics* **18**, 425–431 (2024).
8. Qi, H. *et al.* Homogenizing energy landscape for efficient and spectrally stable blue perovskite light-emitting diodes. *Adv. Mater.* **36**, 2409319 (2024).
9. Wei, K. *et al.* Managing edge states in reduced-dimensional perovskites for highly

efficient deep-blue LEDs. *Adv. Mater.* (2024) doi: 10.1002/adma.202412041.

10. Dong, J. *et al.* Multivalent-effect immobilization of reduced-dimensional perovskites for efficient and spectrally stable deep-blue light-emitting diodes. *Nat. Nanotechnol.* (2025) doi:10.1038/s41565-024-01852-6.
11. Gao, Y. *et al.* Highly efficient blue light-emitting diodes based on mixed-halide perovskites with reduced chlorine defects. *Sci. Adv.* **10**, eado5645 (2024).
12. Jiang, Y. *et al.* Synthesis-on-substrate of quantum dot solids. *Nature* **612**, 679–684 (2022).